



Article

Extraction and Physicochemical Characterization of an Environmentally Friendly Biopolymer: Chitosan for Composite Matrix Application

Meryiem Derraz ^{1,*}, Abdelaziz Elouahli ², Chouaib Ennawaoui ^{1,3}, Mohamed Aymen Ben Achour ⁴, Abdelkader Rjafallah ^{1,5}, El Mehdi Laadissi ¹, Hamza Khallok ², Zineb Hatim ² and Abdelowahed Hajjaji ¹

¹ Laboratory of Engineering Sciences for Energy (LabSIPE), National School of Applied Sciences, Chouaib Doukkali University, EL Jadida 24000, Morocco

² Research Team of Energy, Materials and Environment, Department of Chemistry, Faculty of Sciences, University Chouaib Doukkali, EL Jadida 24000, Morocco; zineb.hatim@yahoo.fr (Z.H.)

³ Green Tech Institute (GTI), Mohammed VI Polytechnic University (UM6P), Benguerir 43150, Morocco

⁴ Univ. Polytechnique Hauts-de-France, INSA Hauts-de-France, CERAMATHS—Laboratoire de Matériaux Céramiques et de Mathématiques, F-59313 Valenciennes, France

⁵ Electrical Engineering and Computer Science Faculty, Transilvania University of Brasov, 500036 Brasov, Romania

* Correspondence: derraz.meryiem@gmail.com

Abstract: Chitosan, which is a derivative of chitin, is particularly popular due to its biodegradable and renewable nature. However, the properties of chitosan can be inconsistent due to the extraction process and its natural origin, which poses a challenge to its use in composite materials as a matrix. The properties of chitosan can be tuned by controlling the degree of deacetylation (the extent to which acetyl groups are removed from chitin to form chitosan) and molecular weight. This paper presents a detailed study on the extraction and characterization of chitosan from shrimp shells. The structural thermal and mechanical characterization were studied using several techniques: Fourier-transform infrared spectroscopy, X-ray diffraction, thermogravimetric analysis and differential scanning calorimetry. The intrinsic viscosity and deacetylation degree were determined using various methods. The results showed an average degree of deacetylation of 77%. The chitosan films exhibited a high tensile strength of 43.9 MPa and an elongation at break of 3.14%. The thermal analysis revealed that the films had a glass transition temperature of 88 °C and a maximum thermal degradation temperature of 320 °C. The findings of this research could contribute to the development of chitosan-based materials with improved properties, leading to its wider adoption in the future for composite matrix application. The simple and efficient method used for the extraction and purification of chitosan from shrimp shells makes it a cost-effective and eco-friendly alternative to synthetic polymers.

Keywords: chitosan extraction; deacetylation degree; biopolymer; composite matrix



Citation: Derraz, M.; Elouahli, A.; Ennawaoui, C.; Ben Achour, M.A.; Rjafallah, A.; Laadissi, E.M.; Khallok, H.; Hatim, Z.; Hajjaji, A. Extraction and Physicochemical Characterization of an Environmentally Friendly Biopolymer: Chitosan for Composite Matrix Application. *J. Compos. Sci.* **2023**, *7*, 260. <https://doi.org/10.3390/jcs7060260>

Academic Editor: Francesco Tornabene

Received: 29 April 2023

Revised: 8 June 2023

Accepted: 16 June 2023

Published: 20 June 2023



Copyright: © 2023 by the authors. Licensee MDPI, Basel, Switzerland. This article is an open access article distributed under the terms and conditions of the Creative Commons Attribution (CC BY) license (<https://creativecommons.org/licenses/by/4.0/>).

1. Introduction

Currently, environmentally friendly materials with improved performance that have reached major global applications and that are still being developed include cellulose, chitosan, polyvinyl alcohol (PVA), polylactic acid (PLA), and others [1–3]. Among the most common applications is use as a composite matrix. In a composite, the polymer matrix primarily governs the structure, environmental tolerance, and durability [4–6]. The incorporation of these biobased polymers into the composite greatly improves their mechanical properties such as tensile strength and impact resistance [7–10].

Chitosan is a biodegradable and renewable biological and easy film formation biopolymer. It has significantly impacted research and development in various fields such as chemistry, biology, health, and environment [11–17]. The biocompatibility, biodegradability,

low allergen potential, non-toxicity, and easy film formation ability of chitosan are all exceptional properties that explain the interest in this natural macromolecule, previously regarded as waste. It has been revealed that this low-cost marine co-product can contribute to the development of many commercial products with high added value. Generally, all industrial applications are concerned, from pharmaceuticals to agroalimentary, including the environment, agriculture, textile, printing, and cosmetics [18–20].

Chitosan products require specific purity and physicochemical properties that are highly related to its extraction process. Since residual proteins and pigments can cause side effects, many methods have been developed to prepare chitosan from exoskeletons with high purity. In general, the methodologies published can be categorized into two types: chitosan extracted using chemical methods and using biological methods [21]. The chemical method is the most common in industrial extraction due to the low cost and non-complexity of the extraction process and the equipment used [22]. The method consists of eliminating proteins (deproteination), mineral elements (demineralization), color (bleaching), and acetamide groups (deacetylation).

Chitosan is the partially deacetylated form of chitin, where a fraction of the N-acetyl-D-glucosamine units have been converted to D-glucosamine. The degree of deacetylation (DD), which represents the ratio of deacetylated units to the total number of units, is a crucial structural parameter influencing the physicochemical properties of chitosan. The term chitosan applies to any copolymer with more than 50% DD. Furthermore, the degree of deacetylation not only impacts the physicochemical properties but also plays a significant role in determining the biological properties of chitosan, including its biocompatibility and biodegradability [23–25]. In addition to the degree of deacetylation, chitosan's structure encompasses various model structures, including type-I and type-II crystallites, which exhibit distinct helical conformations. These different crystalline forms contribute to the material's overall architecture and can influence its mechanical behavior and interactions with other molecules or surfaces. It is also noteworthy that chitosan derived from crustacean sources, such as crabs and shrimps, may have a different structure compared to chitosan obtained from microbial sources like fungi. These structural variations can have implications for chitosan's performance and its applicability in different fields [26–28].

The mechanical and thermal properties of chitosan films are essential in determining their suitability for use in composite applications. The mechanical properties of the chitosan films, such as their tensile strength and impact resistance, are crucial in ensuring the durability and performance of the composite material. Furthermore, the thermal properties of the chitosan films are crucial in determining the stability of the composite material at high temperatures. The use of chitosan films in composite applications has the potential to enhance the mechanical and thermal properties of the composite, making it more resilient and reliable. Therefore, understanding the mechanical and thermal properties of chitosan films is critical in developing sustainable and efficient composite materials for various industrial applications [29–40].

In this work, attention will be focused on the extraction of a biodegradable polymer extracted from crustacean carapaces that is more promising as matrices for bio-composites in the future. The important physicochemical properties of chitosan will be determined. These properties affect directly the quality of the chitosan and are highly influenced by the method used in its production and extraction. The deacetylation degree is one of the most important properties. It was determined by three methods: conductometric titration in basic and acid media, pH titration pH second derivative method, and infrared spectroscopy.

2. Materials and Methods

2.1. Raw Material

The different steps we followed to obtain chitosan are presented in Figure 1. The first step describes the extraction of chitin: the shrimp shells (composed mainly of chitin, proteins, and calcium carbonate) are crushed, washed, and treated in a water bath for 4 h with a sodium hydroxide solution (10% *w/v*) in order to eliminate the proteins. After

filtration, the residue is washed with distilled water and then treated with hydrochloric acid (2N) to remove calcium. The latter reacts with the acid, releasing CO₂, according to the following reaction:

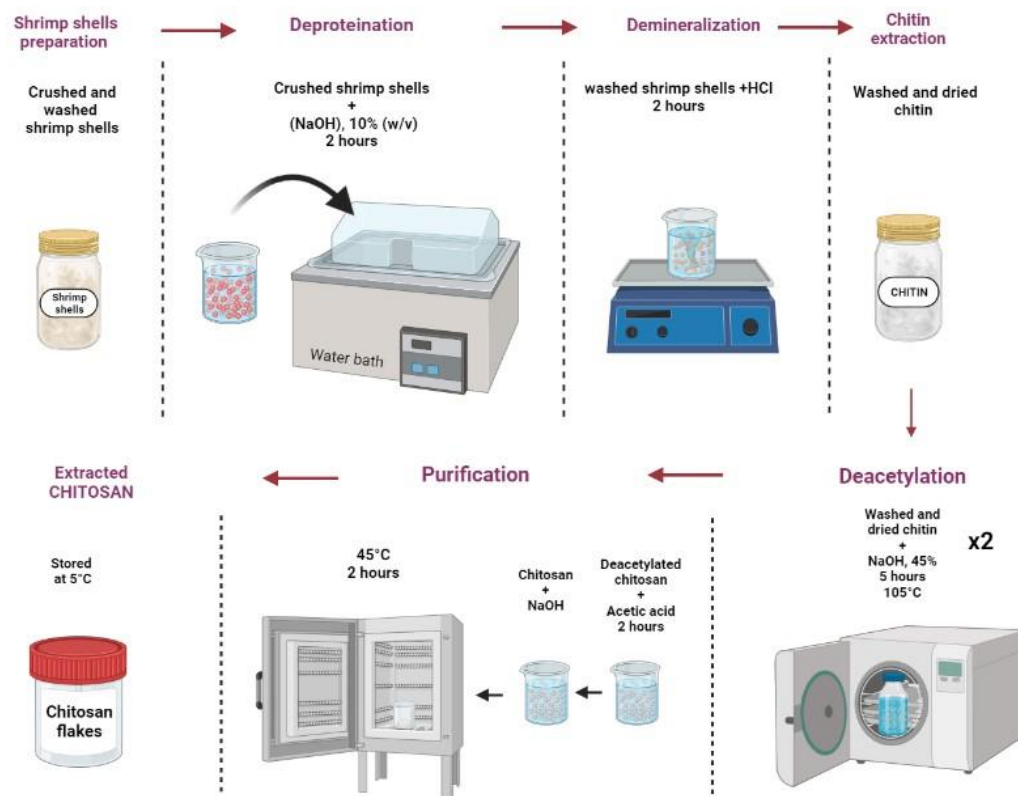
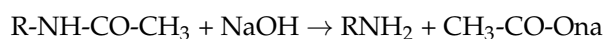


Figure 1. Chitosan extraction protocol by chemical method.

To obtain the chitin, the resulting product was washed with distilled water and ethanol to remove pigments and lipids and then dried. During this treatment process, the color of the shells became lighter and lighter. The obtained chitin thus was white in color, with a fraction of 60 to 70% (by weight) of the quantity of the decalcified carapaces.

To extract chitosan, the chitin is treated in an autoclave with a sodium hydroxide solution (45% *w/v*). The treatment is repeated twice, for 5 h each at a temperature of 105 °C. This operation leads to the deacetylation of the chitin according to the following reaction:



The obtained chitosan is white in color and in the form of flakes representing 85% of the total weight.

To remove any impurities that may have been present in the prepared polymer, we proceeded to the following purification method: a 1% chitosan solution was prepared by dissolving, with agitation, the chitosan flakes in an acetic acid solution at a concentration of 2% by volume. The solution was filtered and the resulting filtrate was neutralized with NaOH (1N) to pH 8. The obtained precipitate was washed abundantly with distilled water and then dried at 45 °C. Finally, the dried chitosan was stored in powder form or in flakes at 5 °C until it was used.

2.2. Chitosan Film Preparation

To prepare the chitosan film we used acetic acid as a solvent. The preparation involved several steps (Figure 2), including dissolving the chitosan powder in acetic acid, casting the

solution onto a substrate, and evaporating the solvent. The chitosan–acetic acid solution was first prepared by dissolving the chitosan powder in acetic acid, typically at a concentration of 2% *w/v*. A homogenous solution was obtained by stirring the mixture continuously at room temperature for a period of 6 h. The solution was then casted on petri dishes at a volume of 25 mL to form a uniform layer, after which the solvent was evaporated by leaving the plate to dry at room temperature.

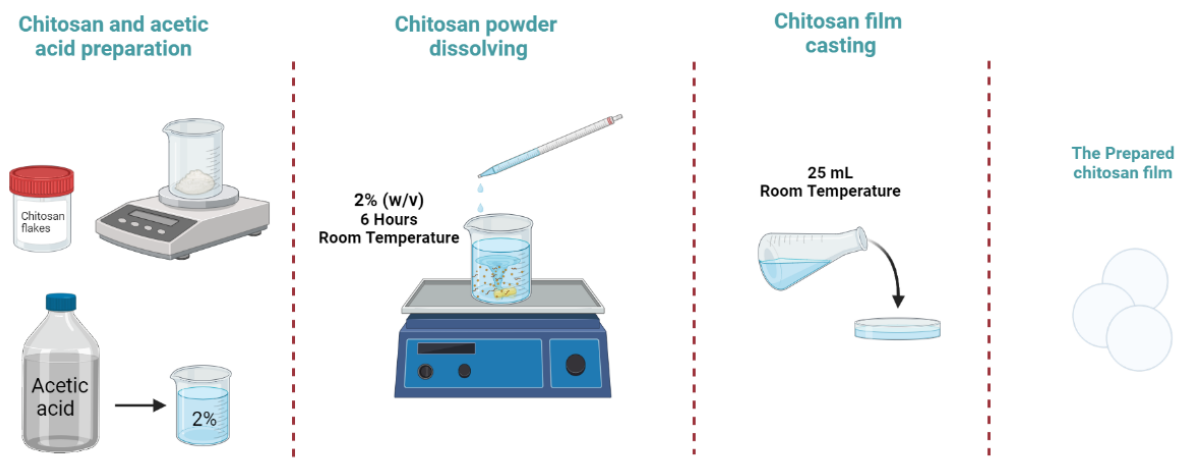


Figure 2. Chitosan film preparation using acetic acid as solvent.

2.3. Characterizations

Fourier-transform infrared spectroscopy was carried out using a spectrometer (Nicolet iS10 Thermo Fisher spectrometer using FTIR) equipped with an attenuated total reflection (ATR) mounting in the wavenumber range between 525 and 4000 cm^{-1} with a resolution of 2 cm^{-1} and with 30 scans. The XRD analysis was carried out using a Bruker advance D8 eco diffractometer, (50 KV-20 mA) equipped with a $\text{CuK}\alpha$ radiation source ($\lambda = 1.5418 \text{ \AA}$). The diffraction patterns were collected over a (2θ) angular range of 10–70°, or 5–70° for the clay fraction, using a size 0.06° (2θ) step and a constant counting time. The chitosan molecular weight was determined based on the intrinsic viscosity. To measure the intrinsic viscosity, we used an Ubbelohde capillary viscometer. The measurement consists of determining, at a given temperature, the flow time in a vertical capillary tube of the same volume of solvent and a chitosan solution. The photoelectric cells are connected to a digital timer giving the flow time in seconds with an accuracy of 10^{-2} s. In order to accurately determine the degree of deacetylation of the prepared chitosan we used three methods: an acid and base conductometric method, a pH-metric method and the IR spectroscopic method. The mechanical properties of the films were determined using tensile testing. A universal tensile machine (MTS criterion model 43) was used for the tests. The tests included measurements of tensile strength (TS) and elongation at break (%E). The samples used were cut into 10 mm \times 4 mm pieces that were tested at room temperature ($26 \pm 1 \text{ }^\circ\text{C}$) with a crosshead speed of 0.1 cm/min. The tensile strength (TS) and the elongation at break (%E) were calculated as follows:

$$\text{TS} = \text{Fmax}/d$$

$$\%E = (\Delta L/L) \times 100$$

where Fmax is the maximum load (MPa), *d* is the average thickness of the film (mm), ΔL is the amount of film extension, and *L* is the initial length of the film.

Thermogravimetry/derivative thermogravimetry (TG/DTG) experiments were performed with a thermogravimetric analyzer (Cahn VersaTherm). The thermal behavior and stability of the chitosan film were assessed at temperatures ranging from 25 $^\circ\text{C}$ to 700 $^\circ\text{C}$, with a heating rate of 20 $^\circ\text{C min}^{-1}$ under a nitrogen atmosphere at a flow rate of 25 mL min^{-1} . Differential scanning calorimetry (DSC) experiments were carried out in a differential scanning calorimeter (SDT-Q600 V8.3) with a controlled cooling accessory.

All materials were sealed in aluminum pans and the DSC scans were performed in a temperature range of 25–400 °C at a heating rate of 10 °C min⁻¹.

3. Results and Discussion

3.1. FTIR and XRD Analysis

Figure 3 shows the FTIR absorption spectra of the prepared chitin and chitosan. The positions of the different vibrational modes observed and their attributions are grouped in Table 1. Both spectra exhibit large vibrational bands located around 3100–3500 cm⁻¹ corresponding to the elongation vibrations of -N-H and -O-H including the hydrogen bonds. The absorbance of this band in the chitosan spectrum decreases in intensity and moves to a higher frequency. The main band at 3383 cm⁻¹ in the chitin spectrum shifts to 3441 cm⁻¹ in the chitosan spectrum. This shift is usually observed when chitosan has a poorly ordered structure.

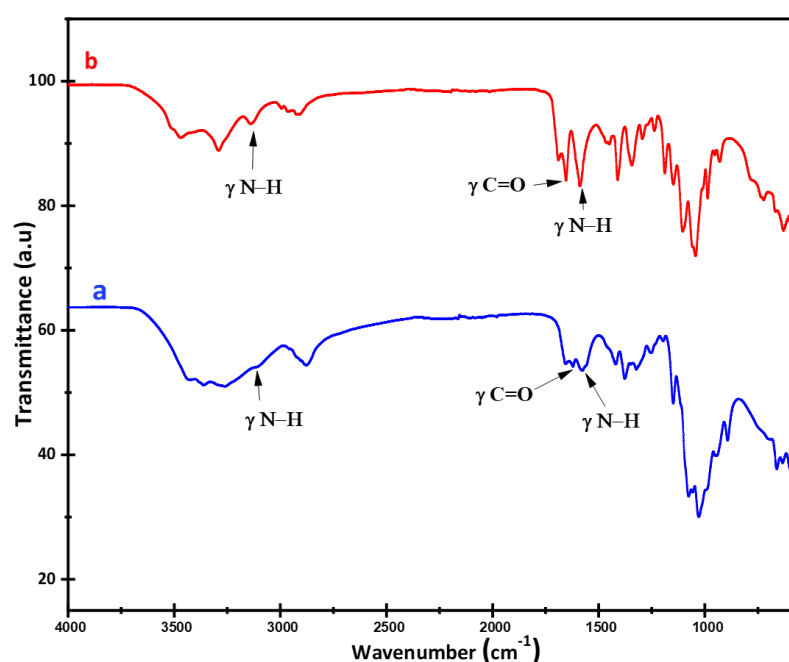


Figure 3. Infrared absorption spectrum of the extracted chitosan (a) and chitin (b).

The absorbances of the bands, due to the elongation vibrations of -CH and -CH₂ at 2880–2923 cm⁻¹, become lower in the case of chitosan.

Two absorption bands are present in both spectra at 1557 and 1652 cm⁻¹ due to the elongation vibrations of -CO-NH₂. These amide I and amide II bands are more easily identifiable in the case of chitin, as the latter is more acetylated than chitosan.

The chitin spectra show bands in the 500–900 cm⁻¹ region known as the structure sensitive region. The absence of these bands in the spectrum of chitosan reflects the change in the structure of the polysaccharide [41].

The absorbances of the bands at 3124 and 3132 cm⁻¹ are lower in the case of chitosan. These absorbances decrease with the increasing degree of deacetylation. This decrease reflects a reduction in the intermolecular hydrogen bonds C(2) N-H...O=C(7) and C(6) OH...HO C(6). These results indicate that the antiparallel arrangements of the chitin chains are transformed into parallel arrangements with the increasing degree of deacetylation [41].

The structural properties of the extracted chitosan were investigated using the XRD technique. The XRD pattern of chitosan is presented in Figure 4, and the peaks observed at 2θ values match the values reported in the literature [42,43]. The pattern shows a broad and poorly defined diffraction peak around 20°, indicating a predominantly amorphous or poorly crystallized structure. The broadening of the peaks can be attributed to the amorphous nature of the polymer. Importantly, no impurity peaks were detected in

the XRD pattern. This structural characteristic can have significant implications for the mechanical properties of the chitosan film. The amorphous or poorly crystallized nature of chitosan typically results in increased flexibility and elasticity, which are desirable traits for various applications [44]. The chitosan film's ability to undergo deformation without fracturing or losing its integrity can be attributed to its poorly crystallized structure. These properties make it suitable for applications where flexibility, tensile strength, and elongation at break are important.

Table 1. Characteristic vibration bends of the extracted chitin and chitosan.

Wavenumber cm^{-1}	Functional Group
500–900	Structure sensitive region
1028	Stretching of the C–O–C of the glycosidic in ring
1089	Stretching of –OH
895 and 1153	Glycosidic bend β (1 → 4)
1254	Distortion vibration of –O–H
1423	Symmetrical deformation of –CH ₃ and –CH ₂
1557	Amide II
1652	Amide I
523.741 and 1652	Chitin identification
2880 and 2923	Elongation of –CH and –CH ₂
3105	Intermolecular hydrogen bending (2) NH..... O=C (7)
3246	Intermolecular hydrogen bending C(6)–OH... HO–C(6)
3100–3500	Elongation of –NH and –OH, including hydrogen bonds

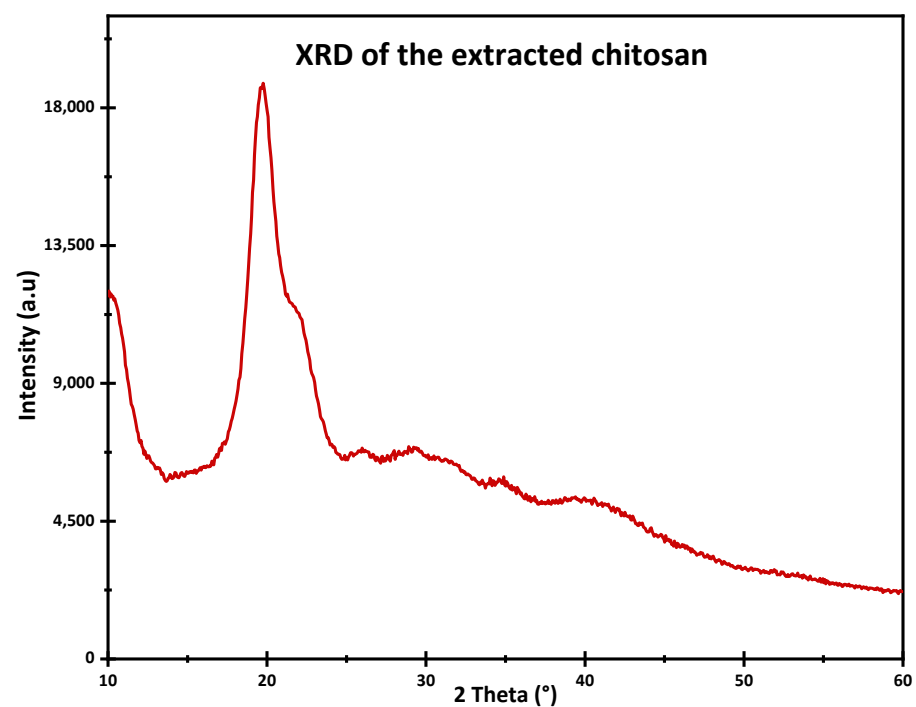


Figure 4. X-ray diffraction of the extracted chitosan.

3.2. Molecular Weight Determination

Chitosan is mainly characterized by its molecular weight, which is an important parameter for a number of its physico-chemical and biological properties such as hydrophilicity, viscosity, water absorption capacity, biodegradability, and biocompatibility. The macromolecular chains of chitosan have a molecular weight in the range of 10 to 1500 kDa. The average molecular weight of chitosan can be determined by a number of techniques, such as osmometry, light scattering, NMR, viscosimetric analysis of the intrinsic viscosity, and chromatographic techniques (size exclusion chromatography, gel permeation chromatography).

One of the most widely used methods for chitosan molecular weight determination is from the intrinsic viscosity η by applying the Mark–Houwink equation:

$$[\eta] = K \cdot M_v^\alpha$$

where:

- K and α are constants that depend on the polymer-solvent system at a given temperature;
- M_v is the molecular weight in dalton (Da);
- η is the intrinsic viscosity.

K and α are the Mark–Howink coefficients whose values are respectively $1.81 \cdot 10^{-3} \text{ mL} \cdot \text{g}^{-1}$ and 0.93 in the case where acetic acid is taken as solvent [45]. The prepared sample had an intrinsic viscosity of 30 cps (measured for 1 g of chitosan in 99 g of acetic acid solution (1%)) and a molecular weight of 700 kDa.

The molecular weight is highly dependent on the chitosan preparation process which may induce depolymerization of the macromolecular chains and/or degradation during its production. The molecular weight value found for the chitosan prepared in this work is relatively higher than those generally given in the literature [46]. This is probably due to the mild treatment used for the deacetylation of chitin. Indeed, the parameters temperature and concentration of the basic solution on the one hand and the autoclave technique on the other hand have an influence on the molecular weight.

3.3. Deacetylation Degree Determination

In order to accurately determine the degree of deacetylation of the extracted chitosan sample, three different methods were utilized. The first method, conductometric titration, involves measuring the change in electrical conductivity as a result of adding a basic solution to the chitosan sample in a solid form. This method provides a measure of the amount of acetyl groups present in the sample, which can be used to calculate the degree of deacetylation. The second method, the pH titration pH second derivative method, is based on the principle that the presence of acetyl groups affects the nitration reaction of chitosan. Finally, the degree of deacetylation was also determined using Fourier-transform infrared (FTIR) spectroscopy. This method measures the infrared spectra of the chitosan sample and compares it to a reference spectrum of fully deacetylated chitosan. In the following sections, we will describe the results obtained using each method and discuss the implications of these results.

3.3.1. Determination of the Degree of Deacetylation by Conductometric Titration

According to Yu et al. [47], conductometric titration is an adequate and appropriate method to determine the degree of deacetylation of chitosan, except for some samples with a high degree of crystallization. This titration method was carried out in basic and acidic media.

- Conductometric titration in basic medium

To investigate the conductivity variation of the chitosan solution, a solution was prepared by dissolving 150 mg of chitosan in 10 mL of hydrochloric acid (0.1 N), and the volume was adjusted to 200 mL using distilled water. The prepared solution was subjected to titration with a sodium hydroxide solution (0.1 N) under continuous stirring. Figure 5

shows the variation of the conductivity of the chitosan solution as a function of the volume of sodium hydroxide added during the titration process.

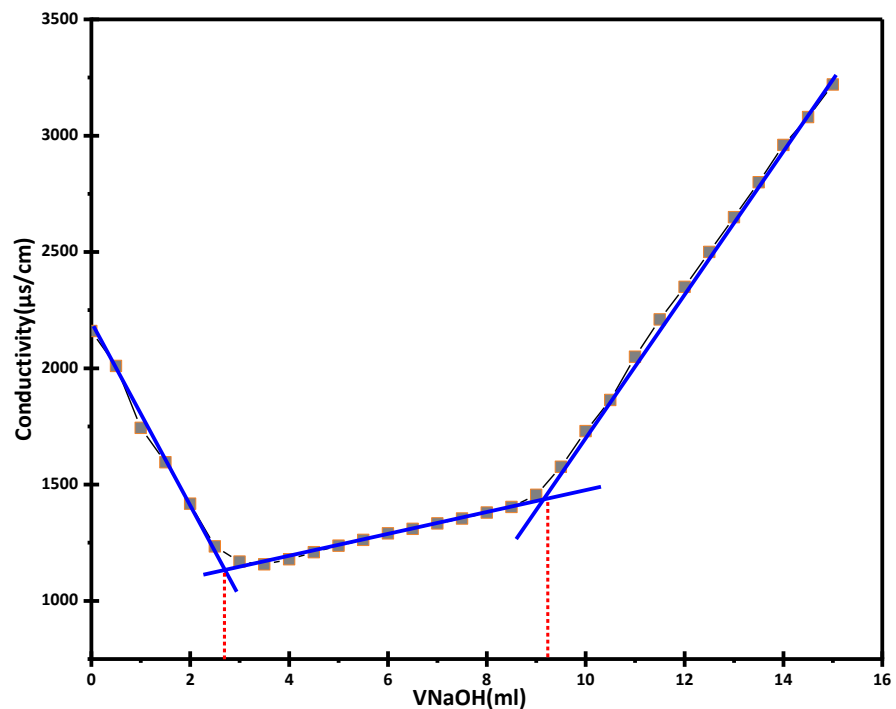


Figure 5. Conductivity variation of the chitosan solution as a function of the volume of a basic solution.

The curve exhibited two distinct inflection points, each representing a significant change in the conductivity. These inflection points correspond to the amount of hydrochloric acid (HCl) required to dissolve the chitosan and convert the amino (-NH₂) groups into ammonium (-NH₃⁺) groups. By measuring the equivalent volumes of NaOH at these points (V₂ and V₁), the degree of deacetylation (DDA) of chitosan can be determined.

The degree of deacetylation (DDA) of chitosan is then calculated from the following equation:

$$DD = 203 \times (V_2 - V_1) \times \frac{N}{m + 42 \times (V_2 - V_1) \times N} \times 100$$

where:

- N is the normality of the NaOH solution (mol·L⁻¹);
- V₂ and V₁ are the equivalent volumes of NaOH representing two inflection points;
- M is the mass of chitosan;
- 203 (g·mol⁻¹) is the molar mass of acetylated monomer;
- 42 (g·mol⁻¹) is the difference between the molecular weight of the acetylated monomer and the molecular weight of the deacetylated monomer.

Applying the conductometric titration method in the basic medium, the calculated degree of deacetylation was found to be DD = 76%.

- Conductometric titration in acid medium

The determination of DD by acid conductometric titration was carried out as follows: A mass of 150 mg of chitosan was dispersed in 200 mL of distilled water, while stirring, and the mixture was titrated with a 0.1 N HCl solution. Figure 6 shows the evolution of the conductivity of the chitosan solution as a function of the volume of HCl added. The inflection point corresponds to the quantity of HCl consumed by the amine groups of the chitosan. The DD was calculated using the following equation:

$$DD = (203 \times V \times N) / (m + 42 \times V \times N) \times 100$$

where:

- N is the normality of the HCl solution ($\text{mol}\cdot\text{L}^{-1}$);
- V is the volume corresponding to the inflection point as shown in Figure 5;
- m is the mass of chitosan (g);
- 42 ($\text{g}\cdot\text{mol}^{-1}$) is the difference between the molecular weight of the acetylated monomer and the molecular weight of the deacetylated monomer.

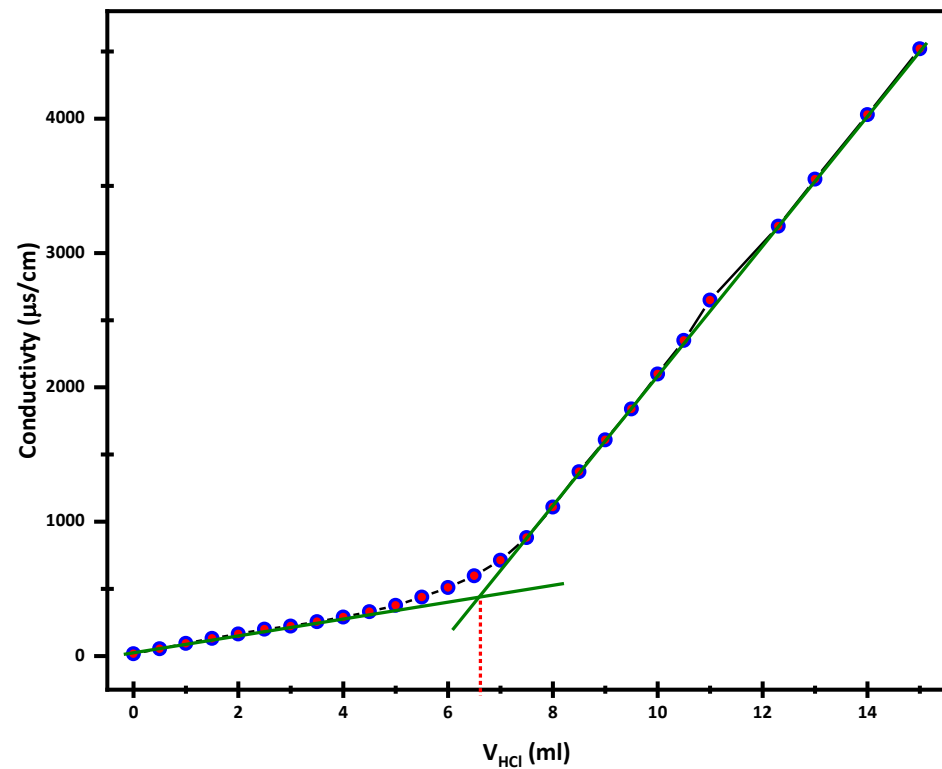


Figure 6. Conductivity variation of the chitosan solution as a function of the volume of acid solution.

The DD determination gives: $DD = 77\%$.

3.3.2. Determination of the Degree of Deacetylation by pH Titration pH Second Derivative Method

The pH titration method is a simple, reliable, and widely used method for determining the degree of deacetylation in chitosan samples. The method is based on the principle that the presence of acetyl groups affects the nitration reaction of chitosan, and the position and height of the peak in the second derivative curve are related to the degree of deacetylation in the sample.

The determination of DD by pH-meter titration was carried out as described in the literature [48–50]. A solution of chitosan was prepared by dissolving 135 mg of chitosan in an excess of HCl (0.1 N) solution and then neutralizing this solution with sodium hydroxide (0.05 N) solution. Figure 7 shows the titration curve for chitosan.

Figure 8 shows the corresponding second derivative. The amount of hydrochloric acid required to protonate the amine groups is determined from the latter curve.

The degree of deacetylation calculated from this method is 77%.

3.3.3. Determination of the Degree of Deacetylation by Infrared Spectroscopy

Infrared spectroscopy has also been used to determine degree of deacetylation [51]. This technique is generally used for qualitative analysis. Quantitative analysis of DD by IR requires well-defined reference bands and an accurately plotted baseline.

The presence of acetyl groups affects the IR spectra of chitosan, and the position and intensity of the IR peaks can be used to identify the presence of acetyl groups in the sample. The DD is calculated from the absorption bands located at 1320 and 1420 cm^{-1} (Figure 9). The first band is characteristic of the acetylated amine or amide function while the second was chosen as the reference band.

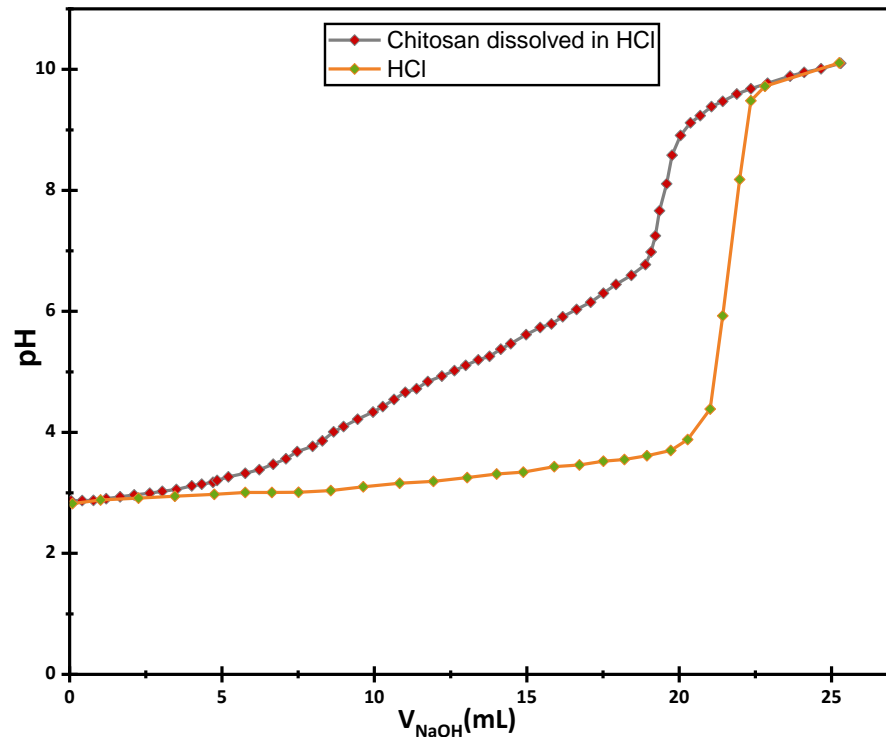


Figure 7. pH variation as a function of the NaOH volume added for the prepared chitosan solution and the HCl solution.

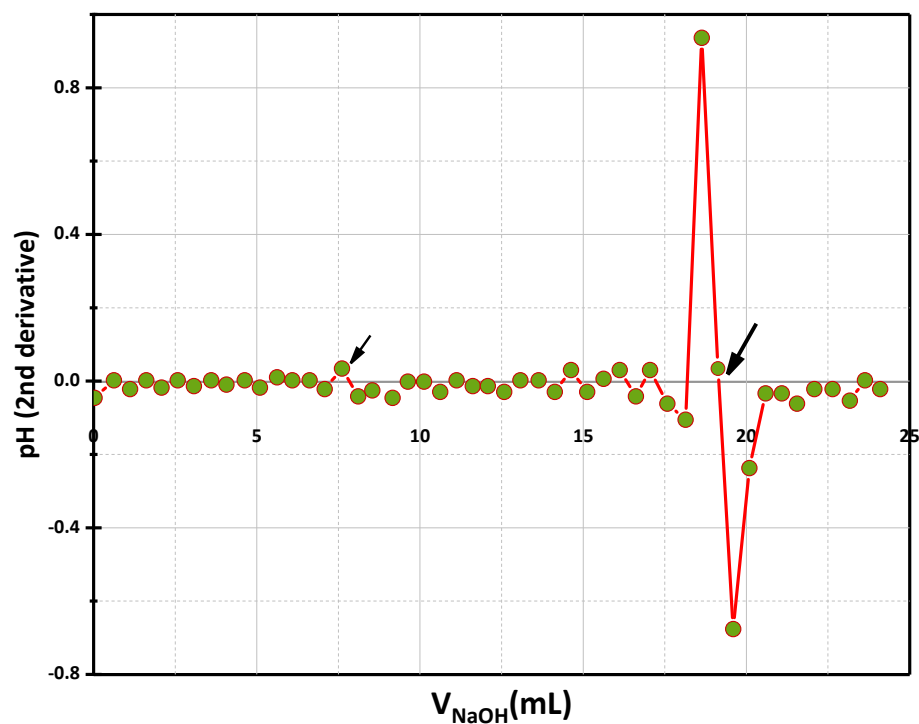


Figure 8. pH secondary derivative curve corresponding to the titration of the prepared chitosan solution.

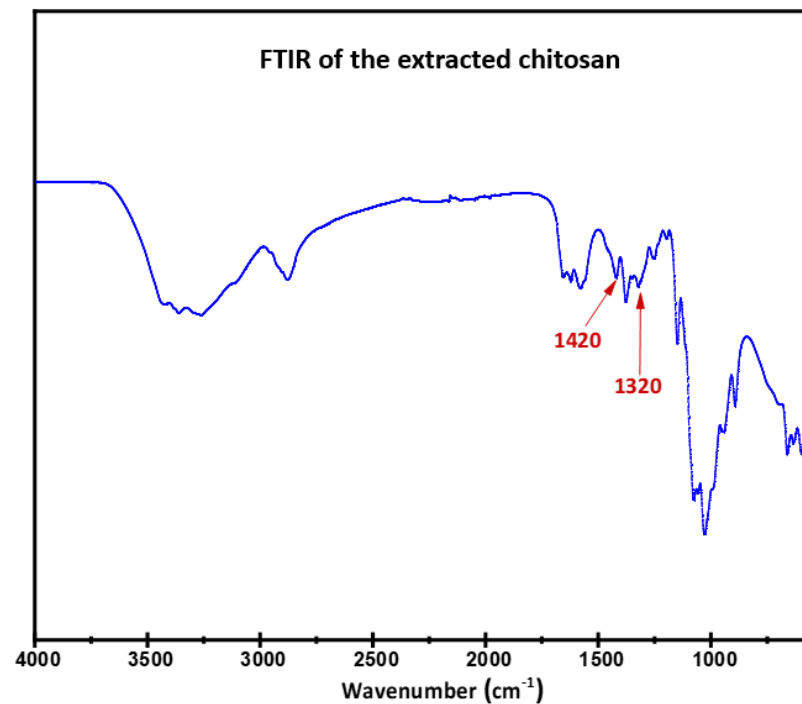


Figure 9. Chitosan infrared absorption spectrum, showing the amide band (1420 cm^{-1}) and the reference band (1320 cm^{-1}).

The equation used to determine the DD of chitosan is the following:

$$\frac{A_{1320}}{A_{1420}} = 0.3822 + 0.03133.(100 - DD)$$

The DD was calculated from this equation to give 78%.

By utilizing multiple methods, we can obtain a more comprehensive understanding of the degree of deacetylation in the extracted chitosan sample. The DDA results obtained by the different titration methods are shown in Table 2. The average DD value calculated for the chitosan prepared in this work is 77%.

Table 2. DD results obtained with different assay methods.

Titration Method	DD %
Conductometric titration (basic)	76
Conductometric titration (acid)	77
pH titration pH second derivative	77
Infrared spectroscopy	78
Average	77

3.4. Mechanical Characterization

Mechanical characterization of chitosan films is crucial in assessing their suitability as a matrix material in composite applications for enhancing mechanical properties. Parameters such as the tensile strength and elongation at break of chitosan films offer valuable insights into the material's ability to withstand external stresses and strains and its behavior under diverse loading conditions.

The chitosan films demonstrated a tensile strength of 43.9 MPa, indicating the maximum stress the material can endure before fracture occurs (Figure 10). Additionally, the

elongation at break was measured to be 3.14%, signifying the maximum strain that the material can undergo before rupturing. These findings indicate the potential of chitosan films to enhance the mechanical properties of composites.

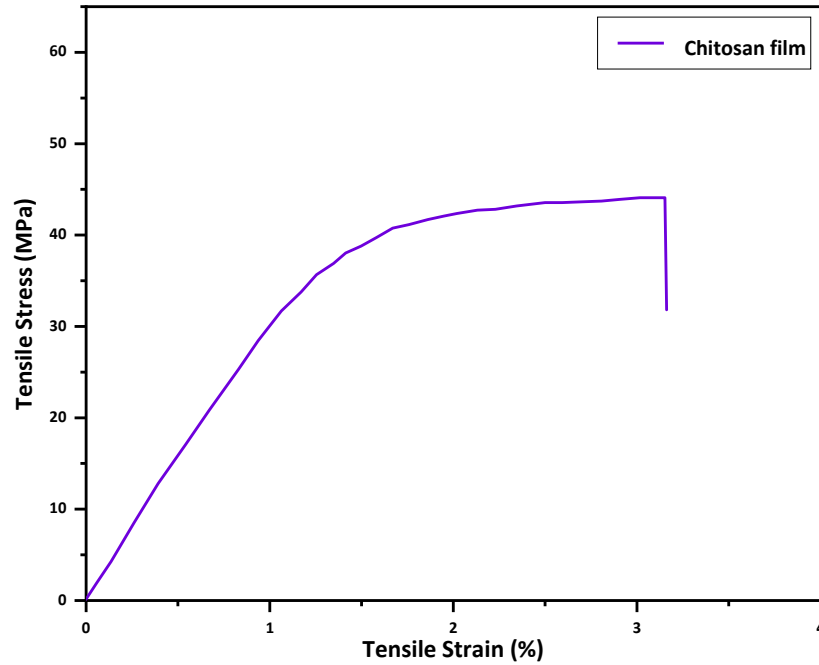


Figure 10. Mechanical analysis: Representative tensile stress × strain test for the prepared chitosan film.

3.5. Thermal Characterization

TG/dTG analysis was performed on the chitosan film to investigate its thermal stability using thermogravimetric analysis. The results (Figure 11) show that the chitosan film had an initial weight loss of about 10% within the temperature range of 50 to 180 °C, which was attributed to water evaporation (moisture content). This was followed by a second weight loss of about 65% at temperatures ranging from 210 °C to 370 °C, which occurred due to saccharide ring degradation, which is in full agreement with the results of previous studies [52,53]. The dTG curve showed a single peak at around 320 °C, which indicated the maximum thermal degradation rate temperature (Tmax). It was observed that the degradation of the chitosan film continued until 450 °C.

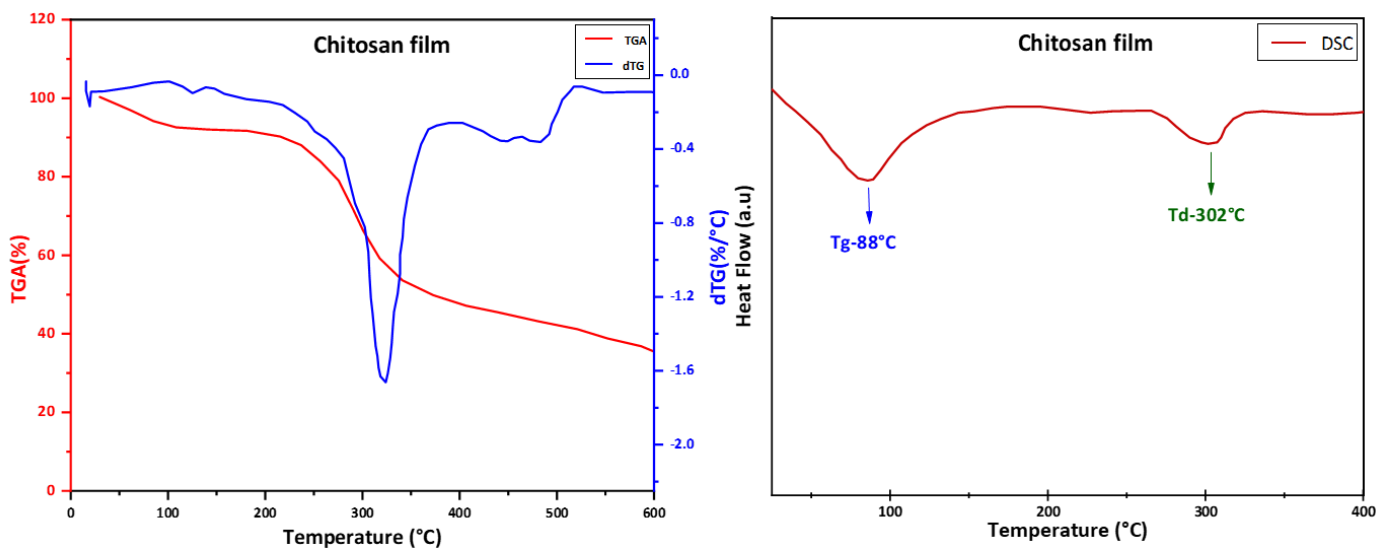


Figure 11. Thermograms: TG and its derivative dTG, and DSC for of the prepared chitosan film.

DSC analysis was also performed on the chitosan films using a differential scanning calorimeter (DSC) to determine the glass transition temperature (T_g) and the thermal degradation temperature (T_d) of the films. The curve (Figure 11) exhibits a first sharp and broad endothermic peak with a maximum at 88 °C, which corresponds to the glass transition temperature (T_g) of chitosan film. The second endothermic peak appeared 302 °C, which corresponds to the thermal degradation temperature (T_d). This result suggests that the chitosan film underwent a two-step degradation process. The first step was the loss of the absorbed water molecules from chitosan, followed by the thermal decomposition of the chitosan polymer. These results align with those reported in the literature [52–54].

Table 3 presents the main characteristics of the prepared sample. The structural characteristics (MW, DD, and viscosity) of chitosan influence its physicochemical and biological properties, such as solubility, biocompatibility, and reactivity, and mechanical properties, such as elongation at break and tensile strength. It has been reported in the literature that high-molar-mass chitosan has the best mechanical and barrier properties compared to low-molar-mass chitosan. Sarasam and Madihally compared three different molar mass ranges of chitosan (50–190 kg/mol, 190–310 kg/mol, and >310 kg/mol) [55]. Their study showed that the tensile strength of chitosan increases with increasing molar mass. As for the degree of deacetylation of chitosan, Wiles et al. (WILES 2000) studied the effect of three degrees of deacetylation of chitosan (92, 84, and 73% DD) on water vapor permeability. They concluded that there is no significant effect on water vapor permeability. It seems that the DD of chitosan affects the bioactivity of chitosan much more than its mechanical properties [56].

Table 3. The prepared chitosan characteristics.

Molecular weight (KDa)	700
Deacetylation degree (%)	77
Intrinsic viscosity (cps)	30
Tensile strength (MPa)	43.9
Elongation at break (%)	3.14
Thermal degradation temperature (°C)	320

4. Conclusions

Chitosan is a promising biopolymer for use as a matrix material in composite applications. The extracted chitosan possesses several desirable properties, including a molecular weight of 700 KDa, a deacetylation degree of 77%, an intrinsic viscosity of 30 cps, a tensile strength of 43.9 MPa, and a thermal degradation temperature of 320 °C. These properties make it suitable for use in various fields, including biomedicine, environmental science, and industry. By controlling the degree of deacetylation, the properties of chitosan-based composites can be enhanced, resulting in improved biodegradability, biocompatibility, and mechanical properties. The mixing of polymers and nanoparticles is opening pathways for engineering flexible composites that exhibit advantageous electrical, optical, or mechanical properties. Moreover, chitosan-based composites have potential applications in food packaging, wound dressings, drug delivery systems, and tissue engineering. Our study highlights the potential of chitosan as a matrix for piezoelectric composite materials. By combining chitosan with piezoelectric materials such as piezoelectric ceramic powder, composite materials with improved piezoelectric properties could be developed. These composite materials have potential uses in areas such as energy harvesting, sensors, and actuators due to their unique properties. Overall, the current body of evidence suggests that chitosan has a promising future as a sustainable and biodegradable material with versatile applications, including as a matrix in composite materials.

Author Contributions: Conceptualization, M.D. and A.E.; methodology, M.D., A.E. and Z.H.; validation, M.D., C.E. and Z.H.; formal analysis, A.E. and C.E.; investigation, M.D. and M.A.B.A.; resources, H.K.; writing—original draft, M.D.; writing—review and editing, C.E. and M.A.B.A.; visualization, A.R. and E.M.L.; supervision, A.H. All authors have read and agreed to the published version of the manuscript.

Funding: This research received no external funding.

Data Availability Statement: The data supporting the findings of this study are available upon request. Researchers interested in accessing the data can contact the corresponding author for further information and to discuss the availability and conditions of data sharing.

Conflicts of Interest: The authors declare no conflict of interest that may be perceived as inappropriately influencing the representation or interpretation of reported research results.

References

1. Cabrera, F.C. Eco-friendly Polymer Composites: A Review of Suitable Methods for Waste Management. *Polym. Compos.* **2021**, *42*, 2653–2677. [CrossRef]
2. Najihi, I.; Ennawaoui, C.; Hajjaji, A.; Boughaleb, Y. 3D Printed Cellular Piezoelectric Polymers for Smart Sensors/Autonomous Energy Harvesters. *Mater. Today Proc.* **2022**, *66*, 437–440. [CrossRef]
3. Najihi, I.; Ennawaoui, C.; Hajjaji, A.; Boughaleb, Y. Theoretical Modeling of Longitudinal Piezoelectric Characteristic for Cellular Polymers. *Cell. Polym.* **2022**, *41*, 39–50. [CrossRef]
4. Aaliya, B.; Sunooj, K.V.; Lackner, M. Biopolymer Composites: A Review. *Int. J. Biobased Plast.* **2021**, *3*, 40–84. [CrossRef]
5. Balazs, A.C.; Emrick, T.; Russell, T.P. Nanoparticle Polymer Composites: Where Two Small Worlds Meet. *Science* **2006**, *314*, 1107–1110. [CrossRef]
6. Ennawaoui, C.; Lifi, H.; Hajjaji, A.; Samuel, C.; Rguiti, M.; Touhtouh, S.; Azim, A.; Courtois, C. Dielectric and Mechanical Optimization Properties of Porous Poly(Ethylene-Co-vinyl Acetate) Copolymer Films for Pseudo-piezoelectric Effect. *Polym. Eng. Sci.* **2019**, *59*, 1455–1461. [CrossRef]
7. Improved Mechanical Properties of Epoxy-Based Composites with Hyperbranched Polymer Grafting Glass-Fiber-Li—2016—Polymers for Advanced Technologies—Wiley Online Library. Available online: <https://onlinelibrary.wiley.com/doi/10.1002/pat.3746> (accessed on 18 April 2023).
8. Zheng, N.; Song, Y.; Wang, L.; Gao, J.; Wang, Y.; Dong, X. Improved Electrical and Mechanical Properties for the Reduced Graphene Oxide-Decorated Polymer Nanofiber Composite with a Core-Shell Structure. *Ind. Eng. Chem. Res.* **2019**, *58*, 15470–15478. [CrossRef]
9. Malki, Z.; Ennawaoui, C.; Hajjaji, A.; Eljouad, M.; Boughaleb, Y. Wave Energy Harvesting System Using Piezocomposite Materials. *Trans. Marit. Sci.* **2022**, *11*, 67–78. [CrossRef]
10. Pedestrian Crossing System for the Mechanical Energy Harvesting Using Piezoelectric Materials—IOPscience. Available online: <https://iopscience.iop.org/article/10.1088/1757-899X/948/1/012030/meta> (accessed on 14 January 2023).
11. Wang, X.; Zheng, K.; Cheng, W.; Li, J.; Liang, X.; Shen, J.; Dou, D.; Yin, M.; Yan, S. Field Application of Star Polymer-Delivered Chitosan to Amplify Plant Defense against Potato Late Blight. *Chem. Eng. J.* **2021**, *417*, 129327. [CrossRef]
12. Shaumbwa, V.R.; Liu, D.; Archer, B.; Li, J.; Su, F. Preparation and Application of Magnetic Chitosan in Environmental Remediation and Other Fields: A Review. *J. Appl. Polym. Sci.* **2021**, *138*, 51241. [CrossRef]
13. Mittal, H.; Ray, S.S.; Kaith, B.S.; Bhatia, J.K.; Sharma, J.; Alhassan, S.M. Recent Progress in the Structural Modification of Chitosan for Applications in Diversified Biomedical Fields. *Eur. Polym. J.* **2018**, *109*, 402–434. [CrossRef]
14. Kato, Y.; Onishi, H.; Machida, Y. Application of Chitin and Chitosan Derivatives in the Pharmaceutical Field. *Curr. Pharm. Biotechnol.* **2003**, *4*, 303–309. [CrossRef]
15. Chopra, L.; Singh Chohan, J.; Sharma, S.; Pelc, M.; Kawala-Sterniuk, A. Multifunctional Modified Chitosan Biopolymers for Dual Applications in Biomedical and Industrial Field: Synthesis and Evaluation of Thermal, Chemical, Morphological, Structural, In Vitro Drug-Release Rate, Swelling and Metal Uptake Studies. *Sensors* **2022**, *22*, 3454. [CrossRef]
16. Aljawish, A.; Chevalot, I.; Jasniewski, J.; Scher, J.; Muniglia, L. Enzymatic Synthesis of Chitosan Derivatives and Their Potential Applications. *J. Mol. Catal. B Enzym.* **2015**, *112*, 25–39. [CrossRef]
17. Xue, C.; Wilson, L.D. An Overview of the Design of Chitosan-Based Fiber Composite Materials. *J. Compos. Sci.* **2021**, *5*, 160. [CrossRef]
18. Kozma, M.; Acharya, B.; Bissessur, R. Chitin, Chitosan, and Nanochitin: Extraction, Synthesis, and Applications. *Polymers* **2022**, *14*, 3989. [CrossRef]
19. Kadouche, S.; Farhat, M.; Lounici, H.; Fiallo, M.; Sharrock, P.; Mecherri, M.; Hadioui, M. Low Cost Chitosan Biopolymer for Environmental Use Made from Abundant Shrimp Wastes. *Waste Biomass Valor* **2017**, *8*, 401–406. [CrossRef]
20. de Menezes, F.L.; Andrade Neto, D.M.; Rodrigues, M.D.L.L.; Lima, H.L.S.; Paiva, D.V.M.; da Silva, M.A.S.; Fechine, L.M.U.D.; Sombra, A.S.B.; Freire, R.M.; Denardin, J.C.; et al. From Magneto-Dielectric Biocomposite Films to Microstrip Antenna Devices. *J. Compos. Sci.* **2020**, *4*, 144. [CrossRef]
21. Kou, S.G.; Peters, L.M.; Mucalo, M.R. Chitosan: A Review of Sources and Preparation Methods. *Int. J. Biol. Macromol.* **2021**, *169*, 85–94. [CrossRef]

22. El Knidri, H.; Belaabed, R.; Addaou, A.; Laajeb, A.; Lahsini, A. Extraction, Chemical Modification and Characterization of Chitin and Chitosan. *Int. J. Biol. Macromol.* **2018**, *120*, 1181–1189. [[CrossRef](#)] [[PubMed](#)]
23. Zakaria, Z.; Izzah, Z.; Jawaid, M.; Hassan, A. Effect of Degree of Deacetylation of Chitosan on Thermal Stability and Compatibility of Chitosan-Polyamide Blend. *BioResources* **2012**, *7*, 5568–5580. [[CrossRef](#)]
24. Seda Tıǧlı, R.; Karakeçili, A.; Gümüşderelioǧlu, M. In Vitro Characterization of Chitosan Scaffolds: Influence of Composition and Deacetylation Degree. *J. Mater. Sci. Mater. Med.* **2007**, *18*, 1665–1674. [[CrossRef](#)]
25. Foster, L.J.R.; Ho, S.; Hook, J.; Basuki, M.; Marçal, H. Chitosan as a Biomaterial: Influence of Degree of Deacetylation on Its Physicochemical, Material and Biological Properties. *PLoS ONE* **2015**, *10*, e0135153. [[CrossRef](#)] [[PubMed](#)]
26. Fernando, L.D.; Dickwella Widanage, M.C.; Penfield, J.; Lipton, A.S.; Washton, N.; Latgé, J.-P.; Wang, P.; Zhang, L.; Wang, T. Structural Polymorphism of Chitin and Chitosan in Fungal Cell Walls From Solid-State NMR and Principal Component Analysis. *Front. Mol. Biosci.* **2021**, *8*, 727053. [[CrossRef](#)]
27. Saito, H.; Tabeta, R.; Ogawa, K. High-Resolution Solid-State Carbon-13 NMR Study of Chitosan and Its Salts with Acids: Conformational Characterization of Polymorphs and Helical Structures as Viewed from the Conformation-Dependent Carbon-13 Chemical Shifts. *Macromolecules* **1987**, *20*, 2424–2430. [[CrossRef](#)]
28. Ogawa, K.; Yui, T.; Okuyama, K. Three D Structures of Chitosan. *Int. J. Biol. Macromol.* **2004**, *34*, 1–8. [[CrossRef](#)]
29. Kasaai, M.R. Bio-Nano-Composites Containing at Least Two Components, Chitosan and Zein, for Food Packaging Applications: A Review of the Nano-Composites in Comparison with the Conventional Counterparts. *Carbohydr. Polym.* **2022**, *280*, 119027. [[CrossRef](#)] [[PubMed](#)]
30. Kamal, S.; Rehman, S.; Bibi, I.; Akhter, N.; Amir, R.; Alsanie, W.F.; Iqbal, H.M.N. Graphene Oxide/Chitosan Composites as Novel Support to Provide High Yield and Stable Formulations of Pectinase for Industrial Applications. *Int. J. Biol. Macromol.* **2022**, *220*, 683–691. [[CrossRef](#)]
31. Fu, R.; Cheng, B.; Ji, X.; Ren, Y.; Yang, L.; Wang, G.; Fei, P. Research Progress of the Preparation and Application of Cellulose/Chitosan Composite Materials. *Cailiao Daobao/Mater. Rev.* **2016**, *30*, 124–129.
32. Chadha, U.; Bhardwaj, P.; Selvaraj, S.K.; Kumari, K.; Isaac, T.S.; Panjwani, M.; Kulkarni, K.; Mathew, R.M.; Satheesh, A.M.; Pal, A.; et al. Advances in Chitosan Biopolymer Composite Materials: From Bioengineering, Wastewater Treatment to Agricultural Applications. *Mater. Res. Express* **2022**, *9*, 052002. [[CrossRef](#)]
33. de Marzo, G.; Mastronardi, V.M.; Algieri, L.; Vergari, F.; Pisano, F.; Fachechi, L.; Marras, S.; Natta, L.; Spagnolo, B.; Brunetti, V.; et al. Sustainable, Flexible, and Biocompatible Enhanced Piezoelectric Chitosan Thin Film for Compliant Piezosensors for Human Health. *Adv. Elect. Mater.* **2022**, 2200069. [[CrossRef](#)]
34. Fernandes, S.C.M.; Freire, C.S.R.; Silvestre, A.J.D.; Pascoal Neto, C.; Gandini, A.; Berglund, L.A.; Salmén, L. Transparent Chitosan Films Reinforced with a High Content of Nanofibrillated Cellulose. *Carbohydr. Polym.* **2010**, *81*, 394–401. [[CrossRef](#)]
35. Mohammed, N.S.S.; Harttar, M.A.M.; Ahmad, F. Fabrication of Biopolymer-Based Piezoelectric Thin Film From Chitosan Using Solvent Casting Method. *J. Adv. Res. Appl. Sci. Eng. Technol.* **2022**, *28*, 80–89. [[CrossRef](#)]
36. Derraz, M.; Sabani, E.; Ennawaoui, C.; Loualid, E.M.; Laadissi, E.M.; Balhamri, A.; Hajjaji, A.; Azim, A.E. Morphological and Ferroelectric Characterizations of Porous Poly (Ethylene-co-vinyl Acetate) Copolymer Films Prepared by Coextrusion and Pressing Methods for Pseudo-piezoelectric Effect. *Mater. Today Proc.* **2022**, *66*, 196–201. [[CrossRef](#)]
37. Zeeshan Soomro, A.M.; Cho, S. Design and Fabrication of a Robust Chitosan/Polyvinyl Alcohol-Based Humidity Sensor Energized by a Piezoelectric Generator. *Energies* **2022**, *15*, 7609. [[CrossRef](#)]
38. Anisimov, Y.A.; Cree, D.E.; Wilson, L.D. Preparation of Multicomponent Biocomposites and Characterization of Their Physicochemical and Mechanical Properties. *J. Compos. Sci.* **2020**, *4*, 18. [[CrossRef](#)]
39. Sabzevari, M.; Cree, D.E.; Wilson, L.D. Gas and Solution Uptake Properties of Graphene Oxide-Based Composite Materials: Organic vs. Inorganic Cross-Linkers. *J. Compos. Sci.* **2019**, *3*, 80. [[CrossRef](#)]
40. Ennawaoui, C.; Hajjaji, A.; Samuel, C.; Sabani, E.; Rjafallah, A.; Najihi, I.; Laadissi, E.M.; Loualid, E.M.; Rguiti, M.; Ballouti, A.E.; et al. Piezoelectric and Electromechanical Characteristics of Porous Poly(Ethylene-Co-Vinyl Acetate) Copolymer Films for Smart Sensors and Mechanical Energy Harvesting Applications. *Appl. Syst. Innov.* **2021**, *4*, 57. [[CrossRef](#)]
41. Preparation and Solubility in Acid and Water of Partially Deacetylated Chitins | Biomacromolecules. Available online: <https://pubs.acs.org/doi/abs/10.1021/bm000036j> (accessed on 6 March 2023).
42. Govindan, S.; Nivethaa, E.A.K.; Saravanan, R.; Narayanan, V.; Stephen, A. Synthesis and Characterization of Chitosan–Silver Nanocomposite. *Appl. Nanosci.* **2012**, *2*, 299–303. [[CrossRef](#)]
43. Prashanth, K.V.H.; Kittur, F.S.; Tharanathan, R.N. Solid State Structure of Chitosan Prepared under Different N-Deacetylating Conditions. *Carbohydr. Polym.* **2002**, *50*, 27–33. [[CrossRef](#)]
44. Cai, Z.; Chen, P.; Jin, H.-J.; Kim, J. The Effect of Chitosan Content on the Crystallinity, Thermal Stability, and Mechanical Properties of Bacterial Cellulose—Chitosan Composites. *Proc. Inst. Mech. Eng. Part C J. Mech. Eng. Sci.* **2009**, *223*, 2225–2230. [[CrossRef](#)]
45. Khan, T.A.; Peh, K.K.; Ch'ng, H.S. Mechanical, Bioadhesive Strength and Biological Evaluations of Chitosan Films for Wound Dressing. *J. Pharm. Pharm. Sci.* **2000**, *3*, 303–311.
46. Gupta, K.C.; Jabrail, F.H. Effects of Degree of Deacetylation and Cross-Linking on Physical Characteristics, Swelling and Release Behavior of Chitosan Microspheres. *Carbohydr. Polym.* **2006**, *66*, 43–54. [[CrossRef](#)]
47. Jia-hui, Y.; Yu-min, D.; Hua, Z. Blend films of chitosan-gelatin. *Wuhan Univ. J. Nat. Sci.* **1999**, *4*, 476. [[CrossRef](#)]

48. Tolaimate, A.; Desbrières, J.; Rhazi, M.; Alagui, A.; Vincendon, M.; Vottero, P. On the Influence of Deacetylation Process on the Physicochemical Characteristics of Chitosan from Squid Chitin. *Polymer* **2000**, *41*, 2463–2469. [[CrossRef](#)]
49. Broussignac, P. Chitosan: A natural polymer not well known by the industry. *Chim. Ind. Genie Chim.* **1968**, *99*, 1241–1247.
50. Muzzarelli, R.A.A. *Chitin*; Elsevier: Amsterdam, The Netherlands, 2013; ISBN 978-1-4831-5946-1.
51. Brugnerotto, J.; Lizardi, J.; Goycoolea, F.M.; Argüelles-Monal, W.; Desbrières, J.; Rinaudo, M. An Infrared Investigation in Relation with Chitin and Chitosan Characterization. *Polymer* **2001**, *42*, 3569–3580. [[CrossRef](#)]
52. Kumar, S.; Krishnakumar, B.; Sobral, A.J.F.N.; Koh, J. Bio-Based (Chitosan/PVA/ZnO) Nanocomposites Film: Thermally Stable and Photoluminescence Material for Removal of Organic Dye. *Carbohydr. Polym.* **2019**, *205*, 559–564. [[CrossRef](#)]
53. Kasai, D.; Chougale, R.; Masti, S.; Chalannavar, R.; Malabadi, R.B.; Gani, R.; Gouripur, G. An Investigation into the Influence of Filler Piper Nigrum Leaves Extract on Physicochemical and Antimicrobial Properties of Chitosan/Poly (Vinyl Alcohol) Blend Films. *J. Polym. Environ.* **2019**, *27*, 472–488. [[CrossRef](#)]
54. Pan, Q.; Zhou, C.; Yang, Z.; Wang, C.; He, Z.; Liu, Y.; Song, S.; Chen, Y.; Xie, M.; Li, P. Preparation and Characterization of Functionalized Chitosan/Polyvinyl Alcohol Composite Films Incorporated with Cinnamon Essential Oil as an Active Packaging Material. *Int. J. Biol. Macromol.* **2023**, *235*, 123914. [[CrossRef](#)] [[PubMed](#)]
55. Sarasam, A.; Madihally, S.V. Characterization of Chitosan–Polycaprolactone Blends for Tissue Engineering Applications. *Biomaterials* **2005**, *26*, 5500–5508. [[CrossRef](#)] [[PubMed](#)]
56. Wiles, J.L.; Vergano, P.J.; Barron, F.H.; Bunn, J.M.; Testin, R.F. Water Vapor Transmission Rates and Sorption Behavior of Chitosan Films. *J. Food Sci.* **2000**, *65*, 1175–1179. [[CrossRef](#)]

Disclaimer/Publisher’s Note: The statements, opinions and data contained in all publications are solely those of the individual author(s) and contributor(s) and not of MDPI and/or the editor(s). MDPI and/or the editor(s) disclaim responsibility for any injury to people or property resulting from any ideas, methods, instructions or products referred to in the content.